

213

**Institut
de Physique
Nucléaire
de Lyon**

Université Claude Bernard

IN2P3 - CNRS

LYCEN 9934
April 1999

**W^+W^- cross-section and W mass measurement
with the DELPHI detector at LEP**

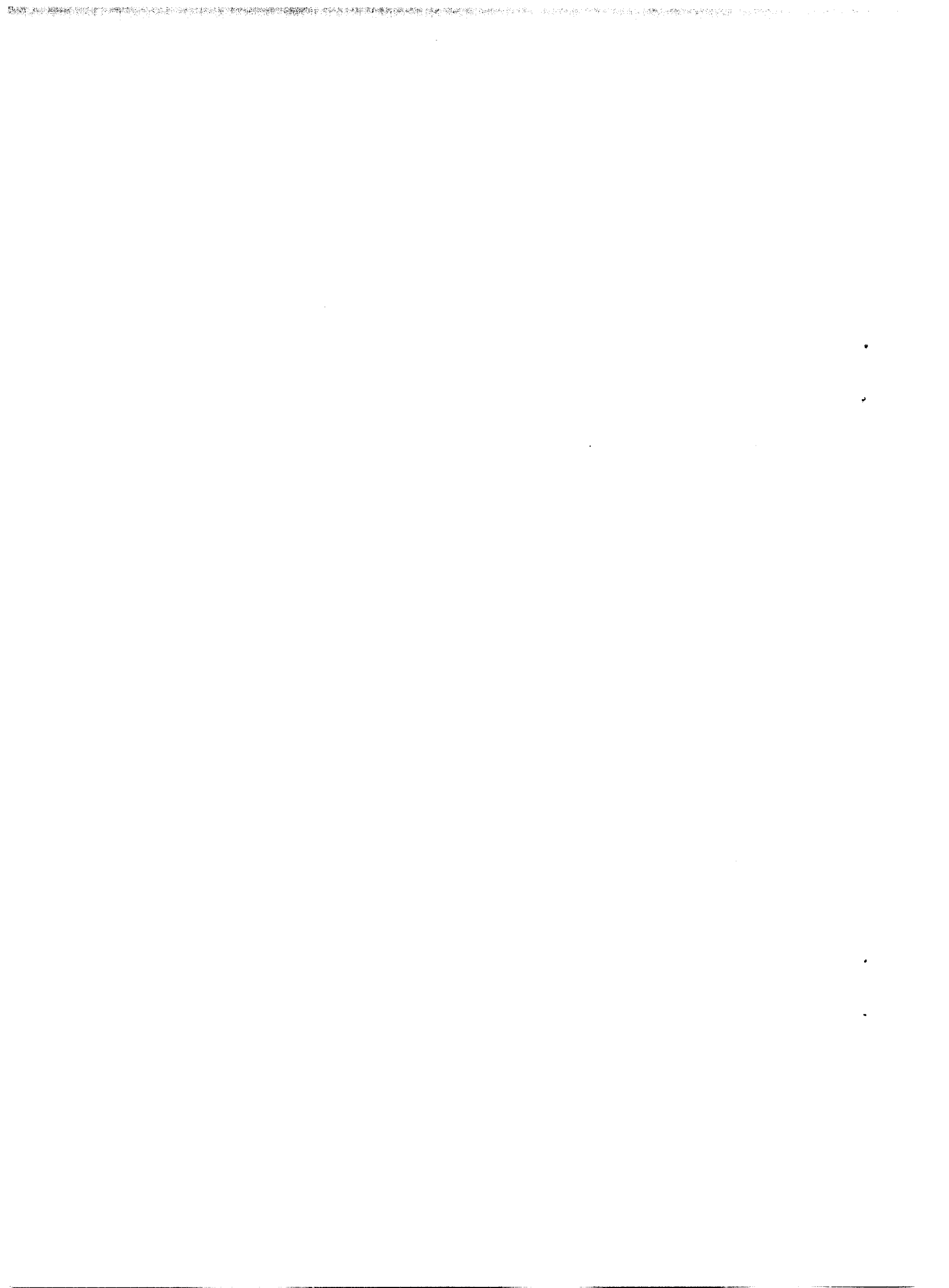
A. Duperrin

Presented at Lake Louise Winter Institute on Electroweak Physics, Alberta,
Canada, 14-20 February, 1999

SCAN-9906055



CERN LIBRARIES, GENEVA



W⁺W⁻ CROSS-SECTION AND W MASS MEASUREMENT WITH THE DELPHI DETECTOR AT LEP

A. DUPERRIN

*Université Claude Bernard de Lyon, IPNL, IN2P3-CNRS,
F-69622 Villeurbanne Cedex, France
E-mail: duperrin@in2p3.fr*

This document reviews the methods and the results for the W⁺W⁻ cross-section and W mass measurement using the data collected up to 1999 with the DELPHI detector.

1 Introduction

The LEP2 programme started in the second half of 1996. The energy was first set at 161 GeV, the most favorable energy for the measurement of the W mass, M_W , from the cross-section for $e^+e^- \rightarrow W^+W^-$ at threshold. The energy was then gradually brought up to 172, 183, 189 GeV leading to an integrated luminosity of about 230 pb⁻¹ in total for DELPHI which is one of the four detectors at LEP. The luminosity measurement is monitored by the Small-Angle Bhabha Scattering $e^+e^- \rightarrow e^+e^-$, a process with large statistics and small theoretical uncertainties. The energy will be increased up to a maximum of about 200 GeV to be reached in mid '99, and LEP2 has been approved to run until the end of 2000 so far, before the shutdown for the installation of the LHC. The main goals of LEP2 are the search for the Higgs and for new particles, the measurement of M_W and the investigation of the triple gauge vertices WWZ and WW γ . A complete updated survey of the LEP2 physics is collected in ref.¹.

The possibility of performing precision tests is based on the formulation of the Standard Model as a renormalizable quantum field theory preserving its predictive power beyond tree level calculations. When the experimental accuracy is sensitive to the loop effects, the Higgs sector of the Standard Model can be probed. This document reports on the W⁺W⁻ cross-section and W mass measurement which have been performed with the DELPHI detector up to 1999.

2 W properties at LEP2

In the Born approximation, three doubly resonant Feynman diagrams contribute to the $e^+e^- \rightarrow W^+W^-$ process, as shown in fig.1. These minimal tree

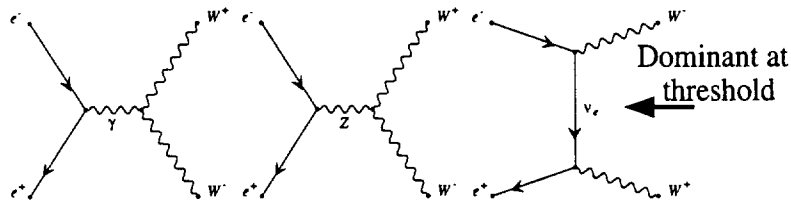


Figure 1. Lowest order Feynman diagrams for $e^+e^- \rightarrow W^+W^-$.

diagrams involve s -channel γ and Z exchange and t -channel ν exchange, the third one being dominant at threshold. Depending on the decay mode of each W , fully hadronic $WW \rightarrow q\bar{q}q\bar{q}$, mixed hadronic-leptonic (“semi-leptonic”) $WW \rightarrow q\bar{q}l\nu$ or fully leptonic final states $WW \rightarrow l\nu l\nu$ are obtained, and the Standard Model branching fractions are 45.9%, 43.7% and 10.4%, respectively. About 3500 W^+W^- pairs were produced in each experiment at LEP2 so far. In addition to their production via the minimal diagrams, the four-fermion final states corresponding to these decay modes may be produced via other diagrams involving either zero, one, or two massive vector bosons. The interference between the three previous diagrams and the additional diagrams are generally expected to be negligible at current energies, except for final states with electrons or positrons. For the W mass reconstruction, the event generator EXCALIBUR² was used for the simulation of all four-fermion final states while the minimal Born processes (including radiatives corrections) were generated with the PYTHIA³ event generator for the cross-section measurement.

This in turn implies that, besides the processes concerning the production and decay of a W -boson pair, one has to consider also those processes that lead to the same final state, but via different intermediate states, called background processes. The main background processes (ZZ , $q\bar{q}(\gamma)$, Zee , $We\nu$...) will be described below in each section dedicated to the three possible WW final states. All final states can be included in the cross-section measurement, while for the mass measurement, only the fully hadronic channel and the three semi-leptonic final states involving an e , a μ or a τ provide enough information. In the fully leptonic final state, the only mass information is given by the charged lepton energy spectrum. As the distribution is considerably smeared, this technique gives a marginal improvement on the mass measurement and has not been implemented.

3 Event selection and cross-sections

The selection of WW events uses the criteria described in detail in ^{4,5} for the cross-section measurements at $\sqrt{s} = 161$ and 172 GeV. In the fully-hadronic final state, however, a neural network analysis has been used for 189 GeV data. These criteria are briefly reviewed in the following sections. The selection for the W mass measurement is similar with slight differences.

The cross-sections are determined for the minimal diagrams. Corrections which account for the interference between the minimal diagrams and the additional diagrams were found to be consistent with unity within the statistical precision of $\pm 2\%$.

3.1 Fully hadronic final state

The event selection criteria were optimized with sequential cuts at $\sqrt{s} = 161$, 172 GeV, 183 GeV in order to ensure that the final state was purely hadronic and in order to reduce the background dominated by electron-positron annihilation into $q\bar{q}(\gamma)$ and ZZ, with a small contamination from $WW \rightarrow q\bar{q}l\nu$. These background processes are generated with the PYTHIA³ event generator. At 189 GeV, a feed forward neural network is used to improve the efficiency \times purity of the selection quality by about 5 %. Input variables are different jet or event observables to characterise $WW \rightarrow q\bar{q}q\bar{q}$ events by high multiplicity, high visible energy, and a four-jet structure. The overall selection efficiency was $90.2 \pm 0.9 \%$ and the cross-section for the expected total background was estimated to be 2.06 ± 0.10 pb. A binned likelihood fit to the distribution of the neural network output variable (figure 2), corresponding to 1340 selected events at 189 GeV, leads to the cross-section measurement : $\sigma_{WW}^{q\bar{q}q\bar{q}} = 7.37 \pm 0.26$ (stat.) ± 0.24 (syst.) pb. The dominant contribution to the systematic error comes from the uncertainty on the background and a conservative contribution of 0.20 pb has been added to the systematic error to account for differences with respect to the result of alternative analyses that were performed as a cross-check.

3.2 Semi-leptonic final state

For $WW \rightarrow q\bar{q}l\nu$ events, sequential cuts were applied to keep events with an isolated high energetic lepton in the case where the lepton is a μ or an e , or events with low multiplicity jets if the lepton is a τ . These events are also characterized by hadronic activity in the detector and missing energy. Figure 3 shows the distribution of the momentum of the selected leptons at 189 GeV.

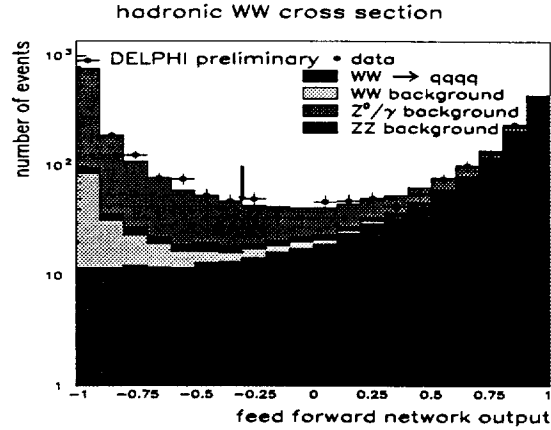


Figure 2. Neural Net output for selection of $WW \rightarrow q\bar{q}q\bar{q}$ events at 189 GeV for the cross-section measurement. The points show the data and the histograms are the predicted distributions for signal (right side) and background (left side). The arrow indicates the cut value.

At this energy, the total event selection efficiency was estimated to be $75.4 \pm 1.4 \%$, for a background contamination of 0.81 ± 0.06 pb. The errors include all systematic uncertainty from efficiency and background determination, the minimal Born diagram correction and measurement of the luminosity. The cross-section result from 906 selected events is: $\sigma_{WW}^{q\bar{q}l\nu} = 6.72 \pm 0.26$ (stat.) ± 0.15 (syst.) pb.

3.3 Fully leptonic final state

These events are characterized by low track multiplicity with a clean two-jet topology with two energetic, acolinear and acoplanar leptons of opposite charge and, by large missing momentum and energy. A total of 188 events was selected at 189 GeV with an overall efficiency of $63.4 \pm 2.3 \%$ and a residual background of 0.155 ± 0.016 pb. The cross-section value from a likelihood fit yields: $\sigma_{WW}^{l\nu l\nu} = 1.68 \pm 0.14$ (stat.) ± 0.07 (syst.) pb (189 GeV). The systematic uncertainty includes track reconstruction efficiency.

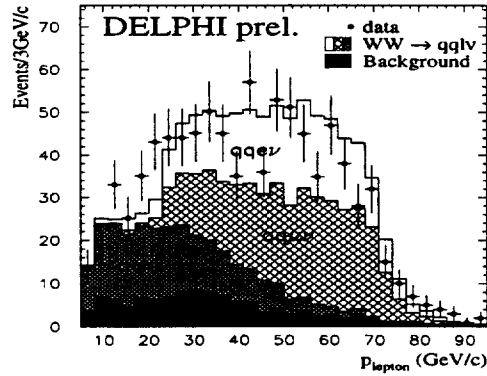


Figure 3. Distribution of the lepton momentum for semi-leptonic events at 189 GeV. The points show the data and the histograms are the predicted distributions for signal and background (dark area).

4 Determination of total cross-section and branching fractions

The total cross-sections for WW production, with the assumption of Standard Model values for branching fractions are shown in table 1 and represented in figure 4. From all final states combined, the branching fractions have been measured. Combining the results at all energies, the results are consistent with lepton universality. Assuming lepton universality, one can derive the leptonic and the hadronic branching fraction. They are shown in table 2. The hadronic branching fraction is in agreement with the Standard Model prediction of 0.677.

5 W mass reconstruction measurement

The event generator EXCALIBUR² was used for the mass measurement. The main points of the analyses both for the $WW \rightarrow q\bar{q}l\nu$ and the $WW \rightarrow q\bar{q}q\bar{q}$ channels are described in ref.^{5,6} for 172-183 GeV data. The results given in the following for 189 GeV are still very preliminary.

| Energy (GeV) | luminosity (pb ⁻¹) | WW cross-section (pb) | stat. error (pb) | syst. error (pb) | (bkg.) (pb) |
|--------------|--------------------------------|-----------------------|------------------|------------------|-------------|
| 161.31 | 10.07 | 3.61 | 0.90 | 0.19 | 0.13 |
| 172.14 | 10.12 | 11.37 | 1.37 | 0.32 | 0.13 |
| 182.65 | 52.52 | 15.86 | 0.69 | 0.26 | 0.10 |
| 188.63 | 154. | 15.79 | 0.38 | 0.31 | 0.09 |

Table 1. WW cross-sections at different centre-of-mass energies. The uncertainty (bkg.) from the QCD background (column 6) is included in the systematic error (column 5). The result at 188.63 GeV is preliminary.

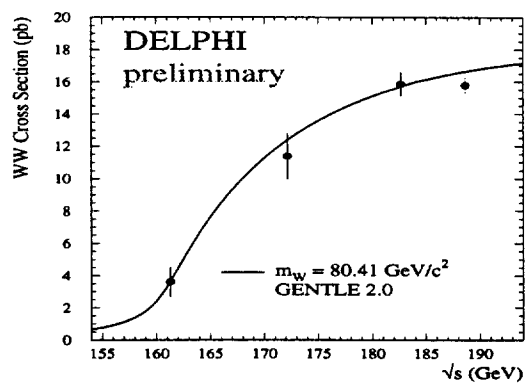


Figure 4. Measurements of the W^+W^- cross-section compared with the Standard Model prediction using $M_W = 80.41 \text{ GeV}/c^2$.

| channel | assuming lepton universality | | | |
|--------------------------------|------------------------------|-------------|-------------|--------|
| | B.R. | stat. error | syst. error | (bkg.) |
| $W \rightarrow \ell\nu$ | 0.1068 | 0.0024 | 0.0019 | 0.0006 |
| $W \rightarrow \text{hadrons}$ | 0.6796 | 0.0073 | 0.0058 | 0.0018 |

Table 2. W branching fractions from the combined 161, 172, 183 and 189 GeV data. The uncertainty from the QCD background (column 5) is included in the systematic error (column 4).

5.1 Reconstruction of the mass in the semi-leptonic and fully hadronic decay channels

- The $WW \rightarrow q\bar{q}l\nu$ channel :

Events were selected using sequential cuts from the data sample recorded while all detectors essential to this measurement were fully efficient. The criteria used to tag the $WW \rightarrow q\bar{q}l\nu$ are similar to those described above for the cross-section measurement. They rely on lepton identification and isolation cuts. After the selection, 88 electron and 109 muon candidates remained in the data at 183 GeV. The number of expected events from simulation is 80.2 with a purity of 91.0% in the electron channel and 100.7 with a purity of 94.5% in the muon channel.

A kinematic reconstruction is applied to obtain an optimal resolution on the 4-momenta of the jets for the mass reconstruction. Energy and equality of the two reconstructed masses is required leading to a two constraints fit. The distribution of the reconstructed masses is shown in figure 5 for real and simulated data in the electron and muon channels. The W mass was extracted

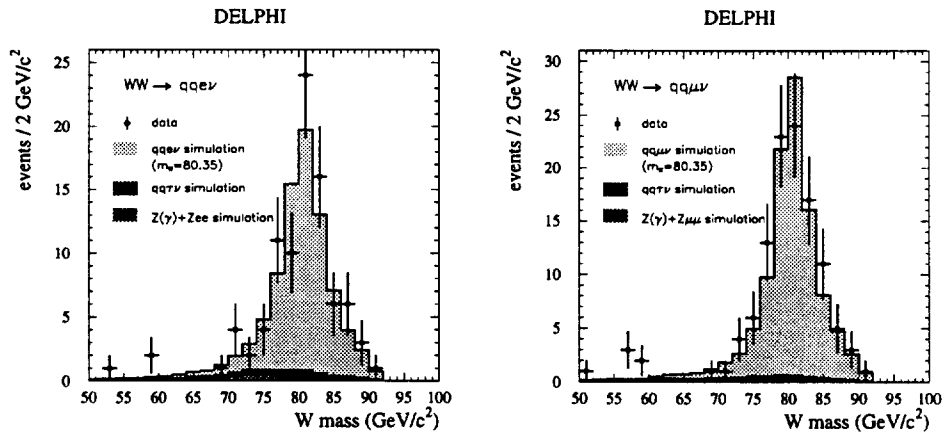


Figure 5. The distributions of the reconstructed masses for the electron and muon channels at 183 GeV.

from the reconstructed mass distribution using the same method for 172, 183 and 189 GeV : an event-by-event maximum likelihood fit to a relativistic Breit-Wigner convoluted with a Gaussian resolution function plus a background

shape. The background distribution was taken from the simulation. The error on the reconstructed mass from the constrained kinematic fit was used as the width of the Gaussian for the corresponding event. Only events in the mass range between 69 and 91 GeV/c² were used in the fit. The events with good resolution have much impact using this method. However, the parametrisation adopted is approximate since detector and physics effects, such as initial state radiation, are not all taken into account. A calibration curve is needed to correct the bias which is estimated with various sample of known generated masses. The same procedure is necessary for the fully hadronic channel.

- The WW → q \bar{q} q \bar{q} channel :

In the fully hadronic channel, the main background contamination comes from the Z → q \bar{q} (γ) events. The priority for the event selection was a high efficiency, rather than a high signal to background ratio, in order to suppress possible bias on the mass determination from a tighter event selection as for the cross-section measurement. With the sequential cuts, efficiency and purity of this selection were estimated to be 88% and 66% respectively at 183 GeV. A total of 540 events were selected from the data (see figure 6). The number of events expected from simulation was 518. However, an independent analysis cross-checked the W mass result using an neural network tagging.

5.2 Event by event likelihood in the WW → q \bar{q} q \bar{q} channel

A constrained fit⁵ was used to improve the precision on the 4-momenta of the jets, requiring energy and momentum conservation. A specific difficulty of the fully hadronic channel (compared to the semi-leptonic channel) comes from the different possible attribution of the jets to each of the two W's. For a four jets event, there are three possible pairing while for a five jets event, this number increases to ten possible associations (two jets for one W and three jets for the opposite W).

To avoid the difficulty of choosing one solution among the different possibilities, the solution adopted is to use all the three and the ten jets solutions. Each solution is then weighted by a probability density function (PDF). The probability density function $p_i(m_x, m_y)$ that this attribution corresponds to two objects with masses m_x and m_y was computed as follows : a 6C-fit with constraints from energy and momentum conservation was performed, fixing the two masses to m_x and m_y , and the probability p_i was derived from the resulting χ^2 of the constrained fit as $p_i(m_x, m_y) \propto \exp(-\frac{1}{2}\chi_i^2(m_x, m_y))$. An example of PDF is shown in figure 6 for a 4-jet event. Further improvements in

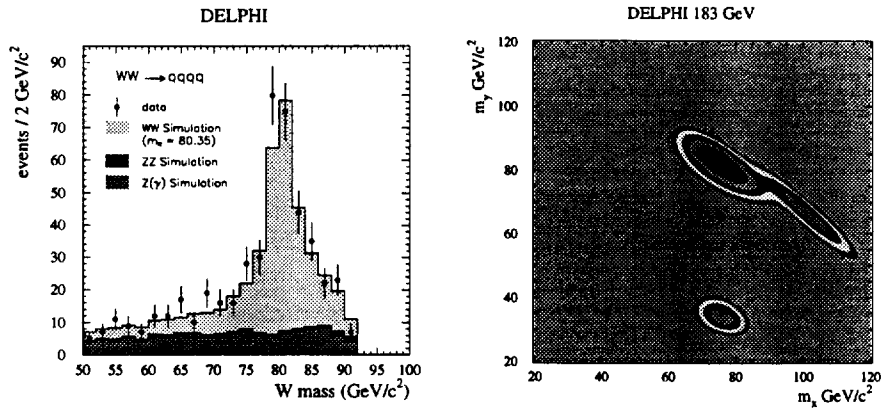


Figure 6. Mass plot (left) for the selected $W^+W^- \rightarrow q\bar{q}q\bar{q}$ candidates at 183 GeV showing only one reconstructed mass per event (that with the best χ^2), and using an equal-mass constraint (not used in the determination of M_W , see text). Examples of probability density function (right) for a 4-jet hadronic event. The first 5 sigma contours are shown. The three possible pairings are clearly distinguishable and the procedure $m_x \simeq 80 \text{ GeV}/c^2$, $m_y \simeq 80 \text{ GeV}/c^2$ has more weight than the two others.

the jet association are implemented which take into account angular distribution between the jets, gluon radiation in five jets events, and results obtained with different jets algorithms.

The W mass result in the fully hadronic channel is cross-checked with an independent analysis at 183 GeV. For this second analysis, a neural network performs both the event selection and the jet assignment. The W boson mass was extracted in this method from a likelihood fit to the two-dimensional plot formed by the average and the difference of the two W-masses obtained with a fast kinematic fit, using the distribution predicted by the full simulation. In order to obtain the Monte Carlo spectrum for arbitrary values of M_W , a Monte Carlo reweighting technique was used. The mass found is in full agreement with the result of the event by event likelihood analysis which is given later.

5.3 Systematic errors

Any error on the simulation will cause a systematic error on the mass. The different sources of systematic errors are discussed in detail in ref.⁵. The list

of the largest ones is presented in table 3.

In the semi-leptonic channel, the dominant systematic effects are due to the uncertainty on the absolute energy calibrations. Bhabha and Compton scattering events showed an uncertainty on the electron energy of 1%, while the systematic uncertainty on the muon momentum was estimated from $Z^0 \rightarrow \mu^+ \mu^-$ events to be 0.5%. The uncertainty on the jet energy was estimated to be 2% from $Z^0 \rightarrow q\bar{q}$ events. In the fully hadronic channel, the present dominant systematic uncertainty comes from interactions among the W decay products (FSI). Since the two W's under LEP2 conditions decay much closer to each other than the typical hadronization scale of 0.5 – 1.0 fm, cross-talk between the two W may lead to systematic error because this is not taken into account in the simulation. Two possible sources of such effects have been identified: colour reconnection (CR) among partons from the two different colour singlet systems and Bose-Einstein correlations (BEC) among identical bosons in the final state. The uncertainty on the LEP beam energy cause an uncertainty which should decrease to about 10 MeV/c² for the forthcoming data taking.

| systematic error (MeV/c) | Electrons | Muons | Leptons | Hadrons | Combined |
|-----------------------------|-----------|-----------|-----------|-----------|-----------|
| Stat. calibrat. | 23 | 18 | 14 | 9 | 8 |
| Lepton energy | 40 | 35 | 26 | - | 9 |
| Jet energy | 50 | 30 | 38 | 20 | 26 |
| Background level | 5 | - | 2 | 5 | 3 |
| Background shape | - | - | - | 5 | 3 |
| Lepton isolat. | 20 | - | 8 | - | 3 |
| Total uncor. | 71 | 50 | 49 | 23 | 29 |
| Fragmentation | 10 | 10 | 10 | 20 | 17 |
| I.S.R. | 10 | 10 | 10 | 10 | 10 |
| Total cor. | 14 | 14 | 14 | 22 | 20 |
| LEP energy | 21 | 21 | 21 | 21 | 21 |
| CR | - | - | - | 50 | 33 |
| BEC | - | - | - | 20 | 13 |
| Tot. FSI | - | - | - | 54 | 35 |

Table 3. Contributions to the systematic error on the W boson mass measurement at 183 GeV. The error sources have been separated into those uncorrelated (uncor.) and correlated (cor.) between the different LEP experiments.

6 W mass combined results

The masses measured in the mixed and hadronic decays analysis are in good agreement within statistics and are displayed in figure 7. Combining results at 161, 172, 183, 189 GeV yields as preliminary W mass measurement :

$$M_W = 80.342 \pm 0.078 \text{ (stat.)} \pm 0.051 \text{ (syst.) GeV}/c^2$$

where (syst.) includes all the systematic uncertainties which have been evaluated so far.

7 Summary and Outlook

The cross-section measurements at 161, 172, 183, and 189 GeV show the clear evidence for the existence of the non-abelian coupling. The measurement of the DELPHI cross-section at 189 GeV is still preliminary : $\sigma_{WW}^{\text{tot}} = 15.79 \pm 0.38 \text{ (stat.)} \pm 0.31 \text{ (syst.) pb}$, this value is 1.5 standard deviations lower than the Standard Model prediction using GENTLE⁷ and assuming a theoretical error of 2 %. The present W boson mass measurement in DELPHI is : $M_W = 80.342 \pm 0.078 \text{ (stat.)} \pm 0.051 \text{ (syst.) GeV}/c^2$. This measurement is compatible with the present world average of the direct mass measurement including TEVATRON and LEP2⁸ : $M_W = 80.410 \pm 0.044 \text{ GeV}/c^2$, but also with indirect mass value from a global electroweak fit : $M_W = 80.364 \pm 0.029 \text{ GeV}/c^2$. The statistical error on the mass is now at the level of the quoted systematics. We therefore need to improve our understanding of the systematic error both for detectors and physics effects. Future new measurements of the W mass with an integrated luminosity more than $\mathcal{L} \simeq 300 \text{ pb}^{-1}$ are expected soon and we should achieve a final LEP2 statistical error below 25 MeV/c² combining results from the DELPHI detector with those of ALEPH, L3, and OPAL experiments.

References

1. G. Altarelli, T. Sjöstrand and F. Zwirner, *Physics at LEP2*, CERN 96-01 (1996) Vol.1.
2. F. A. Berends, R. Pittau and R. Kleiss, *Comp. Phys. Comm.* 85 (1995) 437.
3. T. Sjöstrand, *Comp. Phys. Comm.* 82 (1994) 74.
4. DELPHI Collaboration, P. Abreu et al., *Phys.Lett.* B397 (1997) 158.
5. DELPHI Collaboration, P. Abreu et al., *E. Phys. J.* C2 (1998) 581.

DELPHI W MASS (161+172+183+189 GeV)

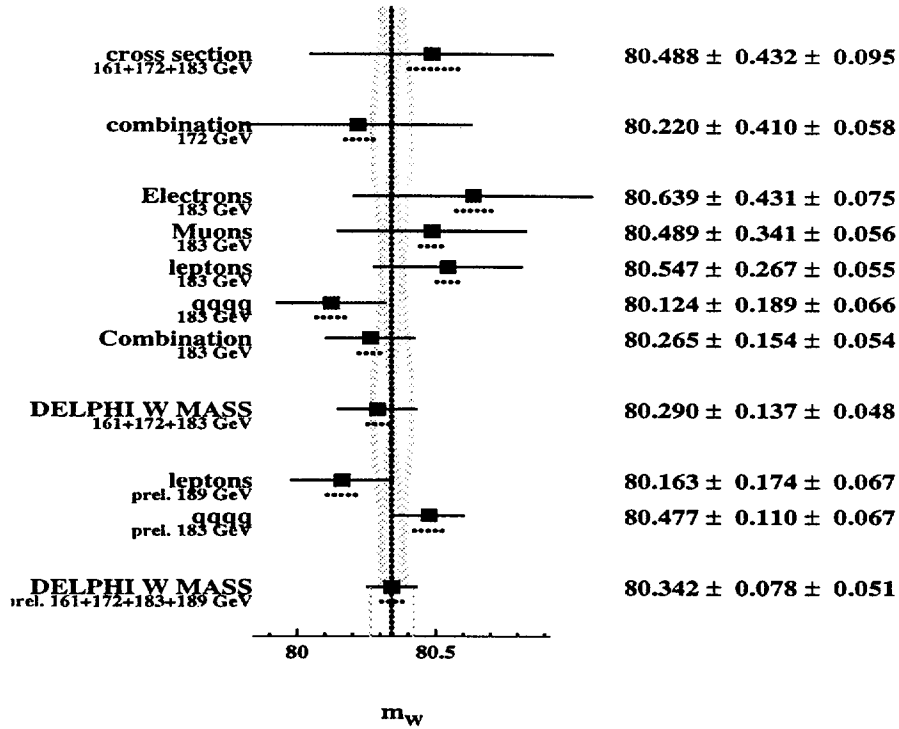


Figure 7. Summary of the DELPHI W mass measurements both in the semi-leptonic channel and the fully hadronic channel for the year 1996-1998.

6. DELPHI Collaboration, P. Abreu et al., 99-41 MORIO CONF 240, *Measurement of the mass of the W boson using direct reconstruction*, (To be submitted to Phys. Lett. B).
7. D. Bardin et al., DESY 95-167 (1995).
8. XXXIVth Rencontres de Moriond, Les Arcs, France, 15-21 March, 1999.
<http://www.cern.ch/LEPEWWG/>,
<http://www.lal.in2p3.fr/CONF/Moriond/ElectroWeak/electroweak.html>